Aspects of Molecular Medicine 5 (2025) 100079

Contents lists available at ScienceDirect

Aspects of Molecular Medicine

journal homepage: www.journals.elsevier.com/aspects-of-molecular-medicine

Structure-based insights into fatty acid modulation of lipid-sensing nuclear receptors PPARδ/γ for glycemic regulation

Shankar Gharge [a,*], Charushila V. Balikai [b], Sachin Gudasi [c]

[a] Department of Pharmaceutical Chemistry, KLE College of Pharmacy, Belagavi, KLE Academy of Higher Education and Research, Belagavi, 590 010, Karnataka, India
[b] Department of Chemistry, SKE Society's Govindram Seksaria Science College, Belagavi, 590006, Karnataka, India
[c] Department of Pharmacognosy, KLE College of Pharmacy, Belagavi, KLE Academy of Higher Education and Research, Belagavi, 590 010, Karnataka, India

ARTICLE INFO

Handling editor: A Angelo Azzi

Keywords:
Diabetes mellitus
Fatty acids
Cluster analysis
SBDD
Molecular dynamics
DFT

ABSTRACT

This study explores the therapeutic potential of fatty acids (FA1-FA12) in the treatment of diabetes mellitus, focusing on their modulation of lipid-sensing nuclear receptors PPARδ/γ. Network pharmacology analysis highlighted key pathways involved in diabetes, including PI3K-Akt, MAPK, and insulin signaling, with targets such as PPAR, INSR, SLC2A4, and AKT1, suggesting a multi-target approach to disease modulation. To investigate their mechanism of action, a pharmacophore model was developed based on the PPAR-γ inhibitor Pioglitazone, offering insights into the essential structural features for ligand binding. Molecular docking studies revealed that FA1 and FA2 exhibited favorable binding affinities at the active sites of both PPAR-γ and PPAR-δ and MD trajectory analysis to evaluate binding orientation and stability of the molecules and the energy profiles of the molecules FA1 (Palmitic acid) and FA2 (Myristic acid), both in complex with the both PPAR-γ and PPAR-δ protein, were assessed. Additionally, computational analyses, including DFT and ADMET predictions, provided valuable information on the electronic and physicochemical properties of the fatty acids. Although these compounds displayed promising lipophilicity and permeability, their poor aqueous solubility indicates the need for optimization in drug development. Overall, this study lays a foundation for the exploration of fatty acids as potential therapeutic agents for diabetes, particularly through their modulation of PPARδ/γ activity for glycemic regulation.

1. Introduction

Diabetes mellitus (DM) is a chronic metabolic disorder characterized by persistent hyperglycemia, which has become a major global health issue (Forouhi and Wareham, 2010). Type II diabetes mellitus (TIIDM), the most common form of the disease, develops due to insulin resistance and insufficient insulin secretion (DeFronzo et al., 2015). This imbalance leads to complications such as dyslipidemia, hypertension, and damage to vital organs like the eyes, kidneys, and cardiovascular system (Mauricio et al., 2020). The increasing prevalence of TIIDM is strongly associated with environmental factors, such as sedentary lifestyles and poor dietary habits, which are further exacerbated by genetic predisposition (Ding et al., 2021). The International Diabetes Federation (IDF) estimates that 537 million adults are currently living with diabetes, a number projected to rise to 783 million by 2045 (McGillicuddy and Roche, 2012; Wang et al., 2022).

One promising therapeutic approach for managing TIIDM involves targeting lipid-sensing nuclear receptors, particularly PPARδ and PPARγ (Gharge et al., 2025; Gharge and Alegaon, 2024). These receptors play critical roles in regulating lipid metabolism, glucose homeostasis, and energy balance, making them attractive targets for developing therapeutic interventions (Agbu and Carthew, 2021). PPARγ, in particular, has gained significant attention due to its key role in adipogenesis, lipid storage, and glucose uptake in tissues such as adipose tissue and the liver (Festuccia et al., 2011). Activation of PPARγ enhances insulin sensitivity, reduces inflammation, and improves lipid metabolism, offering substantial benefits for diabetes management. In contrast, PPARδ, which is primarily expressed in skeletal muscle and adipose tissue, promotes fatty acid oxidation and enhances insulin sensitivity, making it a crucial regulator of metabolic functions (Patil et al., 2024). As a result, both PPARγ and PPARδ represent valuable targets for managing glycemic control and reducing the metabolic complications associated with TIIDM (Gharge et al., 2024a,b,c).

PPARγ has been extensively studied, with several natural and

* Corresponding author.
E-mail address: shankar.gharge135@gmail.com (S. Gharge).

https://doi.org/10.1016/j.amolm.2025.100079
Received 29 December 2024; Received in revised form 15 March 2025; Accepted 16 March 2025
Available online 31 March 2025

synthetic ligands being developed for the treatment of diabetes, obesity, cardiovascular diseases (CVD), and even cancer (Villacorta et al., 2009). Pioglitazone, a well-known PPARγ agonist, has demonstrated significant therapeutic effects, including improving liver function in animal models of renal ischemia-reperfusion and reducing blood pressure by alleviating oxidative and endoplasmic reticulum stress (Mirza et al., 2019). Moreover, PPARα and PPARβ/δ isoforms have gained renewed interest in recent years. Selective PPARβ/δ agonists, such as KD-3010 and Seladelpar, have been tested for non-alcoholic steatohepatitis (NASH), although their clinical approval has been delayed due to their inability to reduce lipid accumulation in hepatocytes (Palomer et al., 2018). On the other hand, PPARα agonists like WY14643 and Fenofibrate have shown promise in treating obesity and hepatic steatosis, while dual PPARα/δ agonists, such as Elafibranor, are currently undergoing phase 3 trials for NASH treatment (Gong et al., 2023). The interplay between these nuclear receptors and the regulation of glucose and lipid

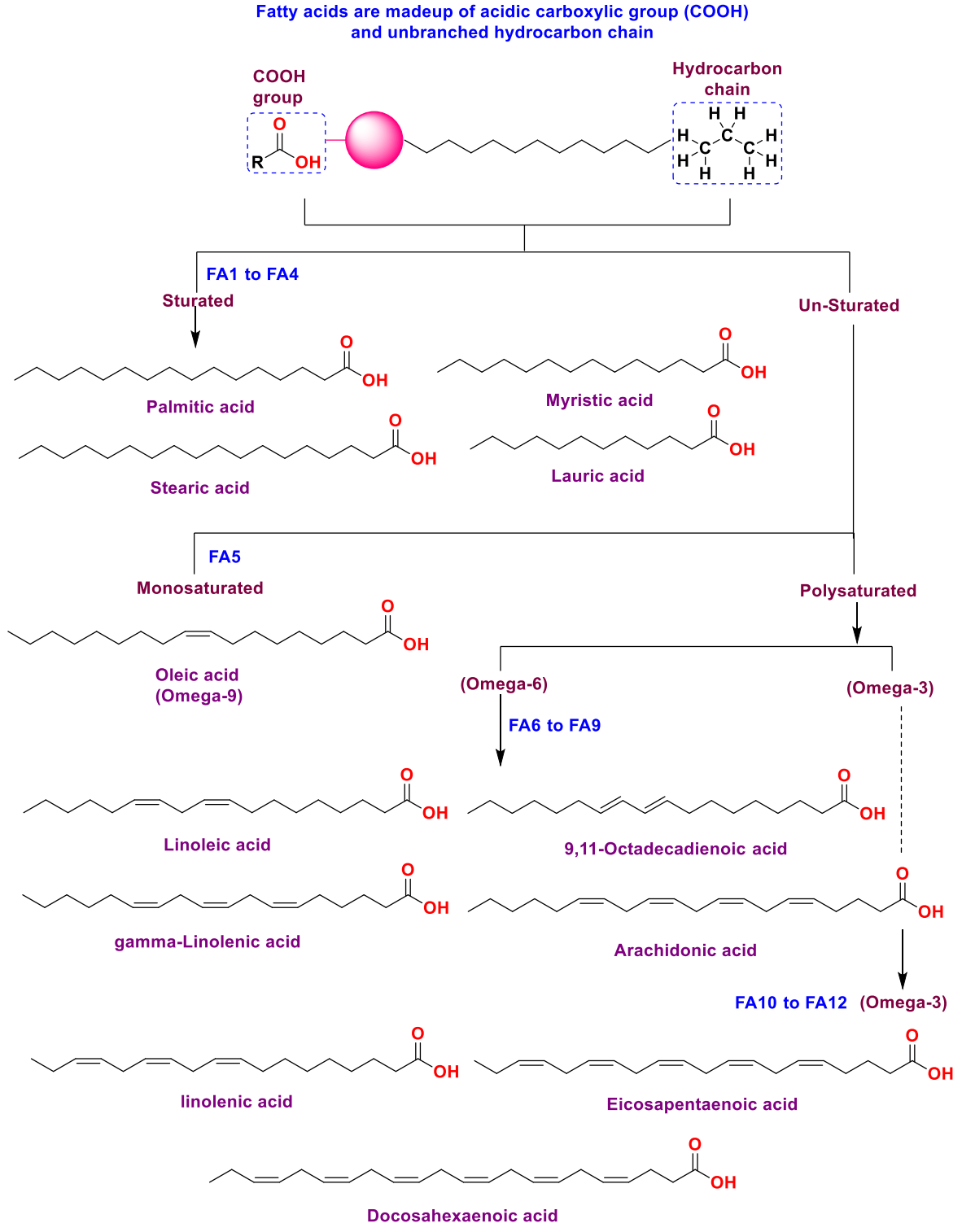

Fig. 1. A visual journey showcasing varying structures and chemical properties of fatty acids.

metabolism is vital for the development of targeted therapies aimed at treating diabetes and associated metabolic disorders.

Fatty acids (FA1 to FA12), essential components of lipids, are crucial for energy storage and cellular functions. Chemically, they consist of long hydrocarbon chains with a carboxyl group (-COOH) at one end. They are classified based on their structure: Saturated Fatty Acids (SFAs) have no double bonds in the hydrocarbon chain, making them solid at room temperature (e.g., palmitic acid, stearic acid). Monounsaturated Fatty Acids (MUFAs) contain one double bond, causing a bend in the chain and making them liquid at room temperature (e.g., oleic acid). Polyunsaturated Fatty Acids (PUFAs) have two or more double bonds, introducing multiple bends that keep them liquid at room temperature, with examples like omega-3 (e.g., EPA, DHA) and omega-6 fatty acids (e.g., linoleic acid). Conjugated Fatty Acids, such as conjugated linoleic acid (CLA), have alternating single and double bonds and are found in meat and dairy products, influencing fat metabolism (Burdge and Calder, 2015; Spector, 1999) Short-Chain Fatty Acids (SCFAs), with fewer than six carbon atoms, are produced by gut bacteria from dietary fibers and play roles in gut health and energy metabolism. The varying structures and chemical properties of these fatty acids significantly impact their biological functions and health effects, fatty acids are currently utilized primarily as dietary supplements rather than stand-alone therapeutic agents for diabetes. (Fig. 1).

These diverse types of fatty acids differ significantly in their chemical structure and functional properties, which in turn affects their roles in health and disease derived from herbal or natural plants are bioactive compounds with diverse therapeutic properties. The ability to modulate lipid-sensing nuclear receptors, such as PPARγ and PPARδ, through structure-based drug design offers a promising avenue for therapeutic interventions (Falomir-Lockhart et al., 2019). By optimizing fatty acid-like molecules to selectively activate or inhibit these receptors, it is possible to enhance insulin sensitivity, improve lipid metabolism, and mitigate associated metabolic complications such as dyslipidemia and inflammation (Shen et al., 2021). Computational approaches, including molecular docking, molecular dynamics simulations, and pharmacophore modeling, are extensively utilized to evaluate ligand interactions with target receptors. This study primarily focuses on in silico analyses to assess fatty acid affinity, potency, and specificity, contributing to the development of potential therapeutic agents for diabetes and metabolic disorders.

2. Materials and methods

2.1. Data set preprocessing

Marketed antidiabetic agents, particularly glitazones, were retrieved from the PubChem database (https://pubchem.ncbi.nlm.nih.gov/). The core structure of fatty acids for this study was designed based on insights from established literature, as depicted in Fig. 1. A series of 12 (FA1 to FA12) congeneric fatty acid molecules were subsequently generated and sketched using the 2D sketcher tool in Maestro 13.2. These molecules were then energy-minimized using the OPLS4 force field to ensure optimized geometry for further analysis.

2.2. Compound-disease-Target-Pathway network construction

In this study, a comprehensive network model was constructed using **Cytoscape 3.7.1** to explore the intricate interactions between components, diseases, targets, and pathways associated with **Diabetes Mellitus**. The model integrated a series of active **fatty acids** (FA1 to FA12) and their corresponding interaction targets to identify key proteins potentially modulated by these compounds. Initially, gene targets associated with Diabetes Mellitus were sourced from the **GeneCards database** (http://www.genecards.org/), which provided a comprehensive list of genes implicated in the disease. In parallel, the genes related to the active fatty acids (FA1 to FA12) were input into the **STRING database** (https://www.string-db.org/), a well-known tool for exploring **protein-protein interactions (PPI)**. The STRING database was used to generate a protein interaction network, which was subsequently visualized and analyzed using **Cytoscape** to uncover potential connections and interactions between fatty acids and targets involved in **Diabetes Mellitus**.

The PPI network was carefully examined and filtered to prioritize the most relevant interactions, focusing specifically on the proteins most likely to serve as therapeutic targets for Diabetes Mellitus. The **cytohubba plug-in** was employed to identify key targets within the network, utilizing node connectivity and betweenness centrality as metrics to determine the importance of each target. Targets with connectivity and betweenness values exceeding the average were considered for further investigation as they may represent critical therapeutic candidates. These top-ranked nodes, which were identified as having a central role in the network, were proposed as key targets for modulation by the fatty acids under study.

To further refine the analysis and gain deeper insights into the biological relevance of the identified targets, **Gene Ontology (GO)** and **Kyoto Encyclopedia of Genes and Genomes (KEGG)** enrichment analyses were performed. The GO analysis provided insights into the associated **biological processes, cellular components**, and **molecular functions** of the identified targets, helping to elucidate the underlying biological mechanisms related to **Diabetes Mellitus**. The KEGG pathway enrichment analysis helped to identify signaling pathways that may be involved in the pathogenesis of the disease and their potential modulation by fatty acids. To visually represent the enriched pathways, a **KEGG enrichment bubble plot** was used, which annotated and highlighted the pathways most strongly associated with Diabetes Mellitus. This visual representation allowed for easy identification of potential therapeutic targets and helped to link the fatty acids to specific biological processes and signaling pathways, this methodology integrates multiple databases and advanced analytical tools to create a comprehensive network model that highlights key targets for **Diabetes Mellitus** and their potential modulation by fatty acids. By utilizing **Cytoscape, STRING, cytohubba**, and enrichment analyses, this study provides a robust framework for identifying therapeutic targets and exploring their connections to the pathophysiology of Diabetes Mellitus, offering insights into potential treatment strategies. The approach utilized in this study is designed to refine our understanding of disease mechanisms and enhance the development of targeted therapeutic interventions for Diabetes Mellitus (Gharge et al., 2024a,b,c; Gudasi et al., 2023).

2.3. Structure based pharmacophore modelling

In this study, cluster analysis revealed that Lipid-Sensing Nuclear Receptors are significantly modulated by the selected fatty acid molecules. To ensure a robust computational analysis, pioglitazone was used as a positive control, while all 12 fatty acids (FA1-FA12) served as potential negative controls in the structure-based drug design (SBDD) approach, following previously established methodologies. This approach enabled a detailed understanding of the molecular features critical for receptor binding and modulation. This method, which combines the benefits of structure-based pharmacophore modeling, generates energetically optimized pharmacophore models. The e-Pharmacophore model was constructed using the PHASE module of the Maestro suite (Gharge et al., 2024a,b,c), identifying six critical pharmacophore features within the active site: hydrogen bond donor (D), hydrogen bond acceptor (A), hydrophobic group (H), aromatic ring (R), positively ionizable (P), and negatively ionizable (N). These features were strategically positioned at chemically relevant locations within the binding site.

Fatty acids (FA1 to FA12) were screened and ranked based on their PHASE screen scores. The three-dimensional structure of the PPAR-γ receptor complexed with the crystal inhibitor 8N6 (Pioglitazone) (PDB

entry 5Y2O) was retrieved from the Protein Data Bank for structure-based pharmacophore generation. The receptor was pre-processed using the Protein Preparation Wizard in Maestro, involving the removal of water molecules and energy minimization (Gharge et al., 2024a,b,c). The active site of the prepared PPAR-γ protein was identified using a 9.0 Å radius sphere, ensuring the inclusion of key residues critical for ligand interactions. This prepared and energetically minimized structure was subsequently utilized for further modeling and analysis.

2.4. In silico study

2.4.1. Molecular docking studies

Docking studies were conducted using Glide's Extra Precision (XP) mode within Schrödinger's suite to examine the binding interactions and orientations of the inhibitors within the PPARδ/γ binding pocket (Gudasi et al., 2024). The XP mode enhances docking accuracy by reducing false positives through advanced scoring mechanisms and comprehensive flexible sampling. The scoring function evaluates multiple interactions, including hydrogen bonds, hydrophobic interactions, and pi-pi stacking. Top ligand (FA1 to FA4) structures were generated using Maestro, and the LigPrep panel was used for ligand preparation, with energy minimization carried out using the OPLS4 force field. The 8N6 (Pioglitazone) crystal inhibitor of *PPAR-γ* (PDB ID: 5Y2O) and D32 (2,3-dimethyl-4-{[2-(prop-2-yn-1-yloxy)-4-{[4-(trifluoromethyl)phenoxy]methyl}phenyl]sulfanyl}phenoxy)acetic acid) crystal inhibitor of *PPAR*-δ (PDB ID: 3GZ9) was obtained from the Protein Data Bank (https://www.rcsb.org) and the protein was prepared using Schrödinger's Protein Preparation Wizard, which involved removing water molecules and generating the grid based on the co-crystal ligand Pioglitazone/8N6 (Gharge et al., 2024a,b,c). Bond orders were assigned, and pKa values were calculated at pH 7 ± 2. To ensure stability for the subsequent docking studies, the protein was then energy minimized using the OPLS4 force field.

2.4.2. Molecular dynamics (MD) simulations

Molecular dynamics (MD) simulations were conducted using Desmond to investigate the structural dynamics of the top fatty acids (FA1 and FA2) within the PPARδ/γ binding pocket. The initial configurations for these simulations were derived from the docking studies, specifically utilizing the Pose Viewer files. To ensure an optimal starting structure, the system was subjected to energy minimization using the OPLS4 force field. The minimization process followed a two-step protocol. Initially, only the water molecules were minimized, while positional restraints were applied to the protein and ligand to maintain their docked conformations. This step helped in optimizing the solvation environment. Subsequently, a full minimization of the entire system was carried out to remove steric clashes and any unfavourable interactions, leading to a well-relaxed initial structure. To create a realistic biological environment, the system was solvated using the TIP3P water model within an orthorhombic box. The box dimensions were set to extend 10 Å beyond the protein in all directions, ensuring complete solvation and sufficient buffering space. To maintain charge neutrality, five sodium ions (Na+) were introduced into the system (Ranade et al., 2024a,b,c). Following minimization, the system underwent a gradual heating phase. The temperature was increased from 0 K to 310.15 K over a span of 100 ps under an NVT (constant number of particles, volume, and temperature) ensemble. During this stage, restraints were applied to the heavy atoms of both the protein and the ligand, allowing the solvent to equilibrate without significant perturbations to the complex. Subsequently, the system underwent density equilibration under an NPT (constant number of particles, pressure, and temperature) ensemble for 1 ns, maintaining a pressure of 1 bar. During this phase, the positional restraints on the protein and ligand were gradually released, allowing the system to reach the desired density and stabilize under physiological conditions.

The final stage of the MD simulation involved a 100 ns production run, ensuring a comprehensive evaluation of the dynamic behavior of FA1 and FA2 within the PPARδ/γ binding pocket. Advanced simulation parameters were employed following predefined conditions to enhance the reliability and accuracy of the results. Throughout the simulation, system properties such as root-mean-square deviation (RMSD), root-mean-square fluctuation (RMSF), hydrogen bonding interactions, and conformational stability were monitored and analyzed to gain insights into ligand-protein interactions and binding stability (Mortier et al., 2015). Overall, this MD simulation approach provided a robust framework for assessing the dynamic behavior and stability of FA1 and FA2 in the PPARδ/γ binding pocket, offering valuable insights into their potential as modulators of this receptor.

2.4.3. Geometric optimization

The energy minimization process was used to predict the most stable molecular conformations, enabling the calculation of bond lengths, angles, and dihedral angles for (FA1 to FA4). Density Functional Theory (DFT), a fundamental computational technique in quantum chemistry, was applied to analyze the electronic structure and properties of the molecules (Ranade et al., 2024a,b,c). Geometric optimization was carried out using the B3LYP functional and the 6-31G (d, p) basis set in the Jaguar module of Schrödinger's software. Additionally, an Electrostatic Potential (ESP) map was generated for each molecule. Quantum chemical parameters such as the energy gap (ΔEGAP), excitation binding energy (ω), dipole moment (μ), hardness (η), and local softness (σ) were calculated based on the values of the highest occupied molecular orbital (EHOMO) and the lowest unoccupied molecular orbital (ELUMO), using standard equations.

$$\Delta E_{GAP} = E_{LUMO} - E_{HOMO} \quad \ldots 1$$

$$\eta = (E_{LUMO} - E_{HOMO})/2 \quad \ldots 2$$

$$\sigma = 1/\eta \quad \ldots 3$$

$$\mu = (E_{HOMO} + E_{LUMO})/2 \quad \ldots 4$$

$$\omega = \mu^2/2\eta \quad \ldots 0.5$$

2.4.4. ADMET profile predictions

The selected fatty acid molecules (FA1 to FA4) were evaluated for their adsorption, distribution, metabolism, excretion, and toxicological (ADMET) properties using the QikProp module of Schrödinger's software (Kavalapure et al., 2021).

3. Results

3.1. GO and KEGG pathway enrichment analysis for PPI network and cluster analysis

A protein-protein interaction (PPI) network was constructed by identifying common targets between fatty acids molecules and known diabetes mellitus targets (Fig. 2). This analysis revealed 51 shared targets, providing a foundation for exploring potential therapeutic strategies. To gain deeper insights into the underlying biological processes and pathways, ClueGO and CluePedia were utilized. These Cytoscape plugins integrate Gene Ontology (GO) and pathway enrichment analyses, offering a visual representation of functionally grouped networks and associated gene/protein interactions. The constructed PPI network identified 805 biological processes and 107 KEGG pathways (Fig. S1). Notably, the KEGG pathways "Type II diabetes mellitus" (KEGG:04930)

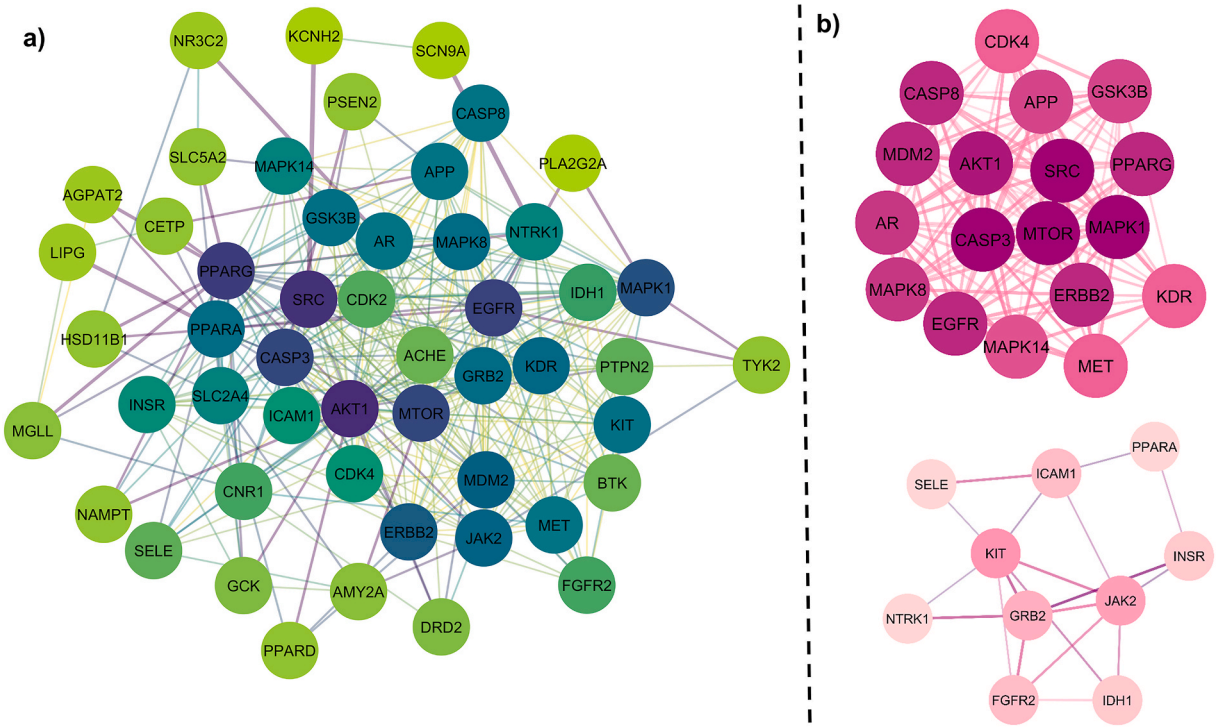

Fig. 2. a) Protein-protein interaction identified for compounds *via* string, b) The cluster analysis where cluster 1: Purple; cluster 2: Pink. (For interpretation of the references to colour in this figure legend, the reader is referred to the Web version of this article.)

and "Insulin resistance" (KEGG:04931) were prominently represented, underscoring their critical roles in the disease. Key genes implicated in these pathways include *GCK, INSR, MAPK1, MAPK8, MTOR, PIK3CB, PRKCD*, and *SLC2A4*, which are involved in glucose metabolism, insulin signaling, and cellular stress responses. The overlap between these pathways, particularly in genes such as *AKT1, GSK3B, INSR, MAPK8, MTOR, PIK3CB, PPARA, PRKCD*, and *SLC2A4*, highlights the central role of impaired insulin signaling and glucose uptake in the pathogenesis of diabetes mellitus (Fig. 2). These findings provide a strong foundation for further investigation of novel therapeutic targets and strategies for the

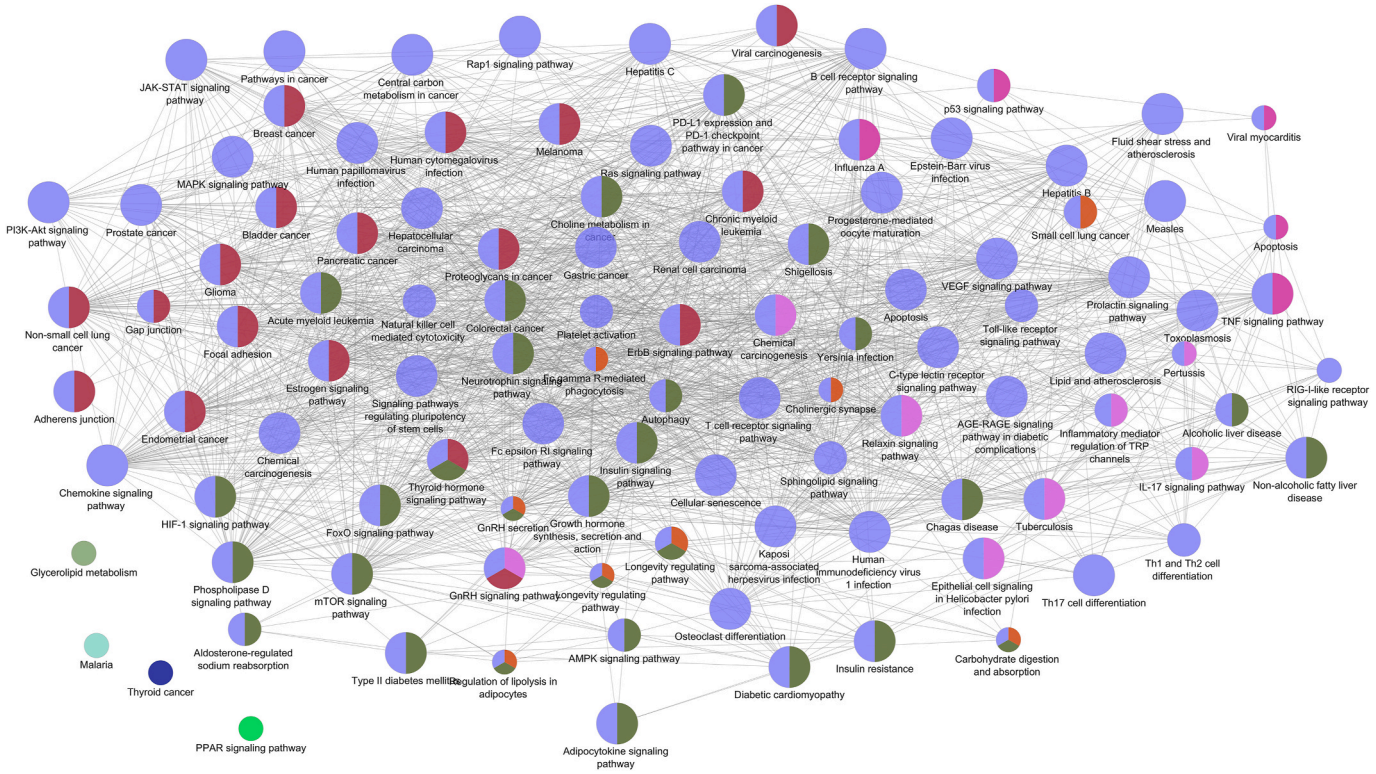

Fig. 3. KEGG Pathway enrichment analysis of PPI Network.

treatment of diabetes mellitus.

MCODE cluster analysis, a topological clustering algorithm, was applied to the PPI network to identify densely interconnected protein modules. This analysis revealed two clusters, with cluster 1 (score = 15.176, 18 nodes, 129 edges) exhibiting the highest score and thus prioritized for further functional and pathway enrichment analysis (Fig. 4). GO enrichment analysis identified 65 biological processes significantly enriched (p-value <0.05) within cluster 1 (Fig. S2 and Fig. S3). Among these, several processes are particularly relevant to diabetes mellitus, including the positive regulation of fat cell differentiation, positive regulation of carbohydrate metabolic process, regulation of mitochondrial membrane potential, positive regulation of cell cycle phase transition, and epidermal growth factor receptor signaling pathway. These mechanisms collectively contribute to glucose homeostasis, insulin sensitivity, and energy metabolism. Furthermore, KEGG enrichment analysis revealed 14 enriched pathways within cluster 1, providing additional insights into the molecular mechanisms involved in diabetes mellitus (Fig. 3).

3.2. Network pharmacology analysis

To elucidate the therapeutic effects of fatty acids in treating diabetes mellitus (DM) at a systems level, network analyses, including Compound-Target (C-T) and Target-Pathway (T-P) interactions, were conducted. A C-T network was constructed using Cytoscape 3.7.1, revealing 156 interactions between 6 compounds and 62 targets. Among the compounds, FA2 (degree = 29) exhibited the biggest number of interactions with the targets, followed by 7b (degree = 25), FA1 (degree = 25), FA3 (degree = 24), FA4 (degree = 23) and FA5 (degree = 23). These compounds with high degrees demonstrated their ability to target multiple receptors, contributing to the interconnected nature of the C-T network. All fatty acids modulated key targets involved in DM, such as *PPAR, GAA, INSR, SLC2A4, PPARD, MAPK1*, and *AKT1*, highlighting their multitargeting potential (Fig. 4). These findings suggest that these compounds may have broad-spectrum effects in treating DM by simultaneously targeting multiple biological pathways.

KEGG pathway analysis was integrated to map all targets and associated pathways into a T-P network using Cytoscape 3.10.1. This network revealed 151 interactions among 47 targets and 21 disease-related pathways with a significance of $P < 0.01$. Notably, the PI3K-Akt signaling pathway was prominently modulated, connecting to 20 nodes including *PIK3CB, AKT1, SLC2A4, INSR, EGFR, MTOR, MAPK1, RAF1, GSK3B, PRKCA, GRB2, MDM2, MET, CDK4, KIT, FGFR2, NTRK1, KDR, ERBB2,* and *CDK2*. MAPK signaling pathway (degree = 18) had the second biggest number of connections with the targets, followed by FoxO signaling pathway (degree = 13) (Mackenzie and Elliott, 2014), insulin signaling pathway (degree = 11) and TNF signaling pathway (degree = 10) (Maiese, 2015). The roles of these high-degree pathways in DM have been well established (REF). Besides, some other pathways also participated in the development of DM, such as mTOR signaling pathway, insulin resistance, Non-alcoholic fatty liver disease and JAK-STAT singling pathway (Fig. 5) (Lampropoulou et al., 2020). In addition, the compounds can also influence many Diabetes mellitus associated pathways, including Fat digestion and absorption, cholesterol metabolism, carbohydrate digestion and absorption, Glucagon signaling pathway and Glycerophospholipid metabolism (Kaltenecker et al., 2019). The specific targets of compounds in this disease associated pathway consider that molecules could exert its therapeutic effects through influencing multiple pathways and acting on multiple targets in each pathway (Yanamadala, 2024). The network pharmacology and enrichment analysis, which predict their interactions with proteins and pathways associated with type II diabetes mellitus and its complications. Fig. 6 illustrates the proposed molecular mechanisms: (A) inhibition of HPA and HLAG and (B) activation of Lipid-Sensing Nuclear Receptors PPARδ/γ for Glycemic Regulation.

Natural ligands for PPARγ, such as the prostaglandin D2 derivative 15-deoxy-Δ12,14-prostaglandin J2 (15d-PGJ2) and oxidized linoleic acid derivatives 9- and 13(S)-HODE, can activate PPARγ in vitro, but their in vivo pathways remain unproven (Marx et al., 2004). Synthetic PPARγ ligands, including thiazolidinediones (glitazones) like troglitazone, rosiglitazone, and pioglitazone, are effective insulin-sensitizing agents used to treat type 2 diabetes by reducing peripheral insulin resistance and lowering blood glucose. While troglitazone was withdrawn due to liver toxicity, rosiglitazone and pioglitazone lack these adverse effects. PPARγ activation in adipose tissue is thought to improve insulin sensitivity by inducing adipogenesis, promoting differentiation of large, insulin-resistant fat cells into smaller, insulin-sensitive ones. This leads to decreased release of free fatty acids and insulin resistance-mediating adipocytokines, such as TNF-α and leptin, alongside increased production of adiponectin, which enhances insulin sensitivity in the liver and skeletal muscle (Fig. 7a).

PPARβ/δ, another lipid-sensing receptor, regulates fatty acid oxidation in muscle and heart tissue. PPARβ/δ agonists have shown promise in normalizing lipid profiles and improving insulin resistance in animal models. Overexpression of PPARβ/δ reverses obesity in mice, suggesting its potential as a therapeutic target for obesity, insulin resistance, and dyslipidemia, with possible vascular benefits (Fig. 7b).

3.3. Structure based pharmacophore modeling

A four-feature (HAAA) e-pharmacophore model was constructed to identify key interactions within the active site of the PPAR-γ protein (PDB ID: 5Y2O) using the crystal inhibitor Pioglitazone (8N6) as a reference. This model, illustrated in Fig. 2, highlights essential structural features required for effective binding and activity, serving as a blueprint for designing new compounds with potential PPAR-γ agonist

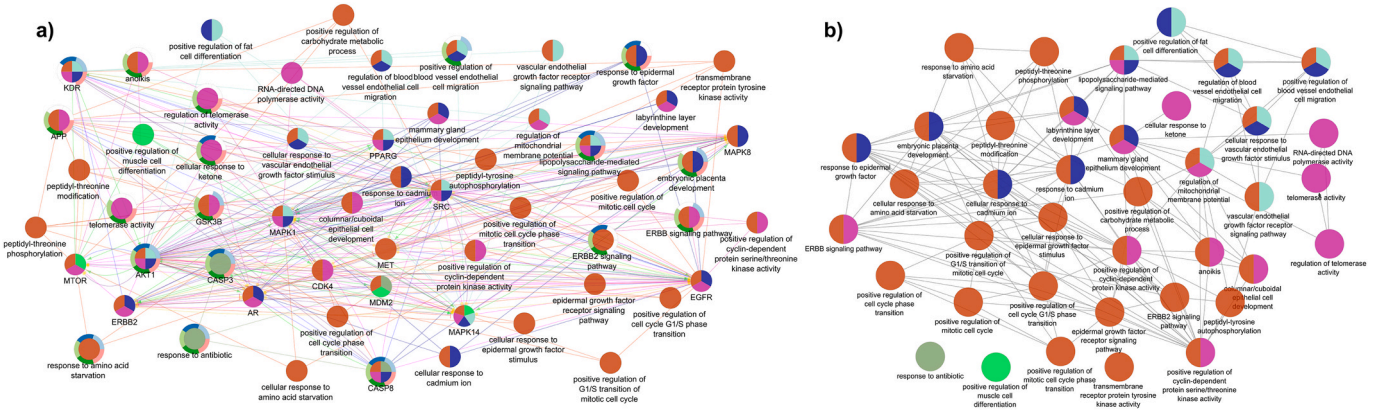

Fig. 4. a) KEGG pathway analysis of the cluster 1, b) Gene ontology (Biological process) enrichment analyses of the cluster 1 by Clue GO plugin.

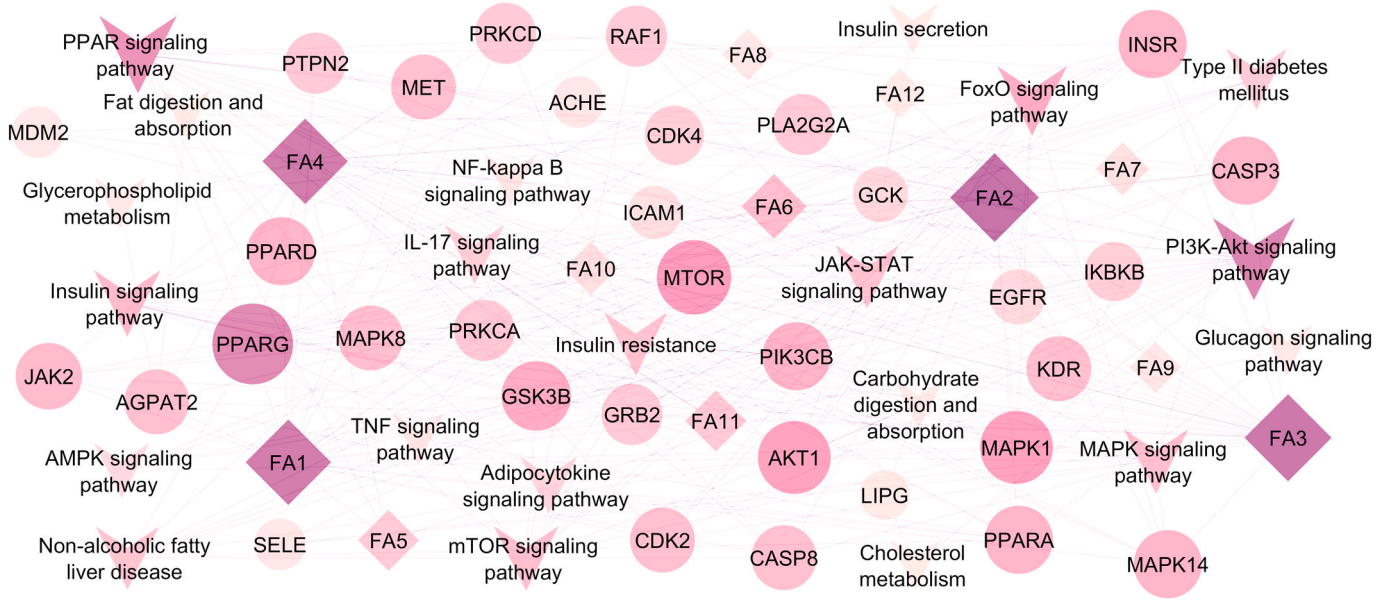

Fig. 5. Compound-disease-target-pathway network construction of fatty acids (FA1 to FA12) involved in TIIDM and respective pathways.

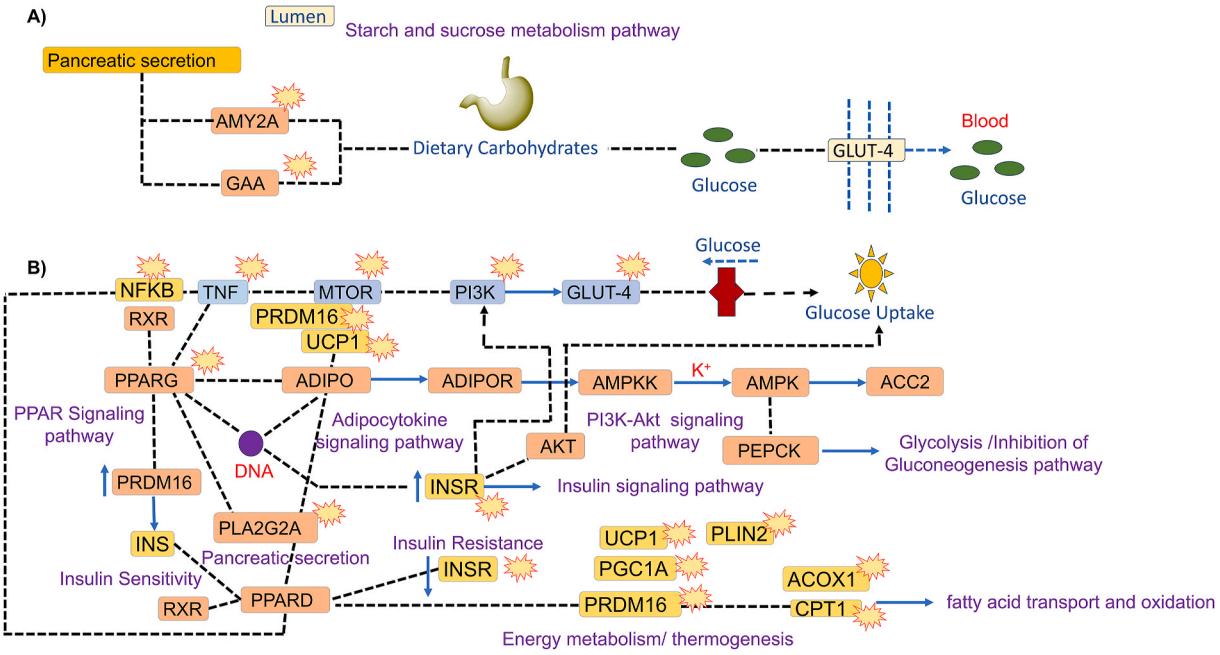

Fig. 6. Probable molecular mechanism of fatty acids in (A) HPA inhibitors (hsa00500, hsa04922, hsa00010), HLAG inhibitors (hsa00500, hsa04922, hsa00010) and (B) Lipid-Sensing Nuclear Receptors PPARδ/γ for Glycemic Regulation (hsa03320), represents checkpoints affected by the compounds in type II DM.

activity. The spatial arrangements, including inter-site distances and angles between pharmacophoric features, are also detailed in Fig. 8, providing critical insights into the structural requirements for PPAR-γ ligands.

The model incorporates three hydrogen bond acceptors (A2, A3, and A4) and one hydrophobic feature (H7). The distances between the acceptors are as follows: A2-A3 (8.41 Å), A3-A4 (4.51 Å), and A2-A4 (9.03 Å). The hydrophobic group is positioned relative to the acceptors as H7-A2 (7.36 Å) and H7-A4 (12.20 Å). Calculated angles include A2-H7 (95.7°), A2-A4 (36.9°), A2-A3 (29.7°), and A3-A4 (67.5°), with A2 serving as the central reference point. These geometric relationships suggest that ligands matching these features may exhibit strong PPAR-γ agonist activity.

A library of fatty acid derivatives (FA1 to FA12) was screened against this pharmacophore model, with enrichment analysis using a decoy set of 1000 molecules (Fig. S4). Among the 12 screened fatty acids, the top four (FA1 to FA4) were ranked based on their fitness scores relative to the reference ligand, as shown in Fig. 9. Compound FA2 emerged as the best candidate, exhibiting five matches with scores of 1.82 for the phase screen, 0.57 for the vector, 0.86 for the alignment, and 0.54 for the volume. The chemical attributes of FA2 include a prominent hydrogen bond acceptor from the oxygen atom of its carboxylic group, which is a critical feature for its observed PPAR-γ agonist activity. These molecular characteristics, combined with its superior pharmacophoric alignment, underscore its potential as a lead compound. The overall strategy, integrating e-pharmacophore modeling, screening, and computational

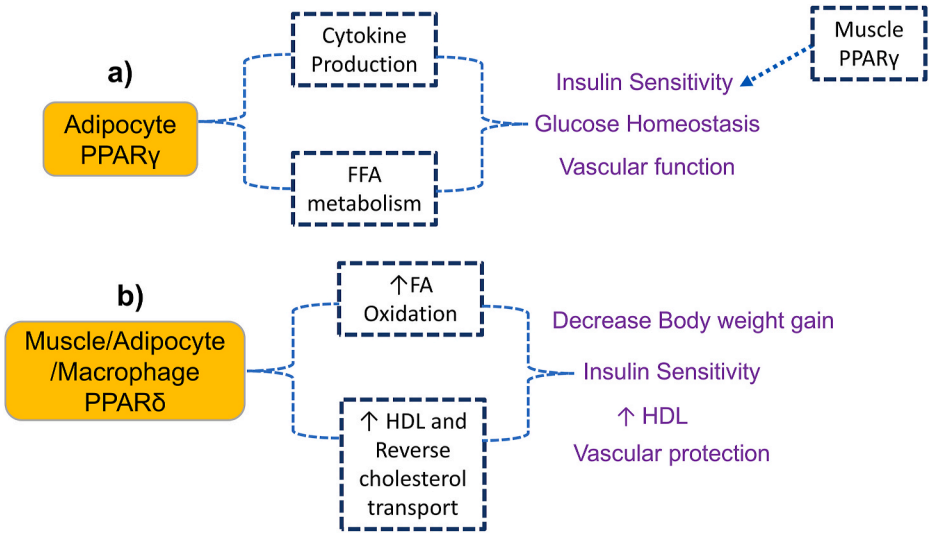

Fig. 7. Metabolic Actions of PPARγ and PPARδ a) In the liver, PPARγ primarily exerts its regulatory effects on adipocytes, influencing insulin signaling, cytokine production, and fatty acid (FA) metabolism. By modulating these processes, PPARγ plays a key role in maintaining glucose homeostasis and may also impact vascular function. Additionally, PPARγ is thought to contribute directly to insulin sensitivity in muscle tissue. b) PPARβ/δ primarily stimulates fatty acid oxidation in muscle, with some effects also observed in adipose tissue. As a result, agonists targeting PPARβ/δ could be beneficial for managing both obesity and insulin resistance.

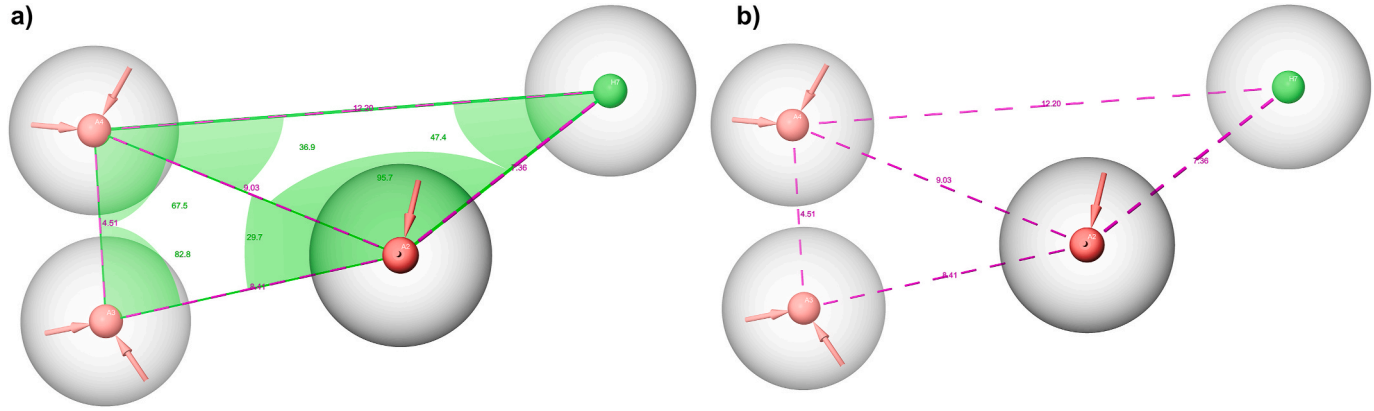

Fig. 8. Inter-site angle (a) and inter-site distance (b) between different features of the developed e-Pharmacophore model. Pink spheres with arrow, hydrogen bond acceptor (A); solid green spheres, Hydrophobic region (H). (For interpretation of the references to colour in this figure legend, the reader is referred to the Web version of this article.)

analysis, is depicted in Fig. 9, illustrating a systematic approach to identifying potent PPAR-γ agonists (see Table 1).

3.4. Molecular docking

The molecular docking study of fatty acid molecules (FA1: Palmitic acid; FA2: Myristic acid; FA3: Stearic acid and FA4: Lauric acid) was performed against the crystal inhibitors of PPAR-γ (8N6, Pioglitazone, PDB ID: 5Y2O) and PPAR-δ (D32, PDB ID: 3GZ9) using the Schrodinger Suite 2020-1. The results, visualized through the Maestro interface, focused on the lipid-sensing nuclear receptors PPAR-γ and PPAR-δ in complex with their respective standard inhibitors. Among the tested molecules, FA1 and FA2 showed the most favorable binding affinities and critical interactions within the active pockets of PPAR-γ and PPAR-δ (Fig. S5 and Table 2).

In the PPAR-γ binding pocket, FA1 exhibited the highest binding affinity of −8.14 with a glide energy of −39.24 kcal/mol, forming hydrogen bonds with TYR473, HIE323, HIE449, and SER289. FA2 followed closely with a binding affinity of −8.02 and a glide energy of −37.05 kcal/mol, interacting with the same residues. FA3 and FA4 displayed slightly weaker affinities of −6.99 and −6.98, respectively, engaging HIE323, HIE449, and SER289. The reference compound, pioglitazone, exhibited superior binding with a binding affinity of −10.57 and a glide energy of −59.11 kcal/mol, interacting with TYR473, SER289, and HIE323 (Fig. 10).

In the PPAR-δ binding pocket, FA2 demonstrated the strongest binding affinity of −11.03 with a glide energy of −41.11 kcal/mol, forming hydrogen bonds with TYR473, HIE323, and HIE449. FA1 showed a binding affinity of −9.64 and a glide energy of −35.74 kcal/mol, engaging TYR473 and HIE449. FA3 and FA4 displayed affinities of −9.10 and −8.87, respectively, interacting with TYR473, HIE323, and HIE449. The reference co-crystal ligand, D32, outperformed all tested molecules with a binding affinity of −10.57 and a glide energy of −59.11 kcal/mol, interacting with TYR473, SER289, THR288, and HIE323 (Fig. 11). The molecular docking study revealed that key amino acid residues, including TYR473, HIE323, and HIE449, are consistently involved in hydrogen bond interactions across all tested fatty acid molecules (FA1–FA4) and the standard inhibitors (Pioglitazone for PPAR-γ and D32 for PPAR-δ). These common residues play a crucial role in the binding stability within the active pockets of PPAR-γ and PPAR-δ, highlighting their importance in ligand-receptor interactions and potential drug design targeting these nuclear receptors.

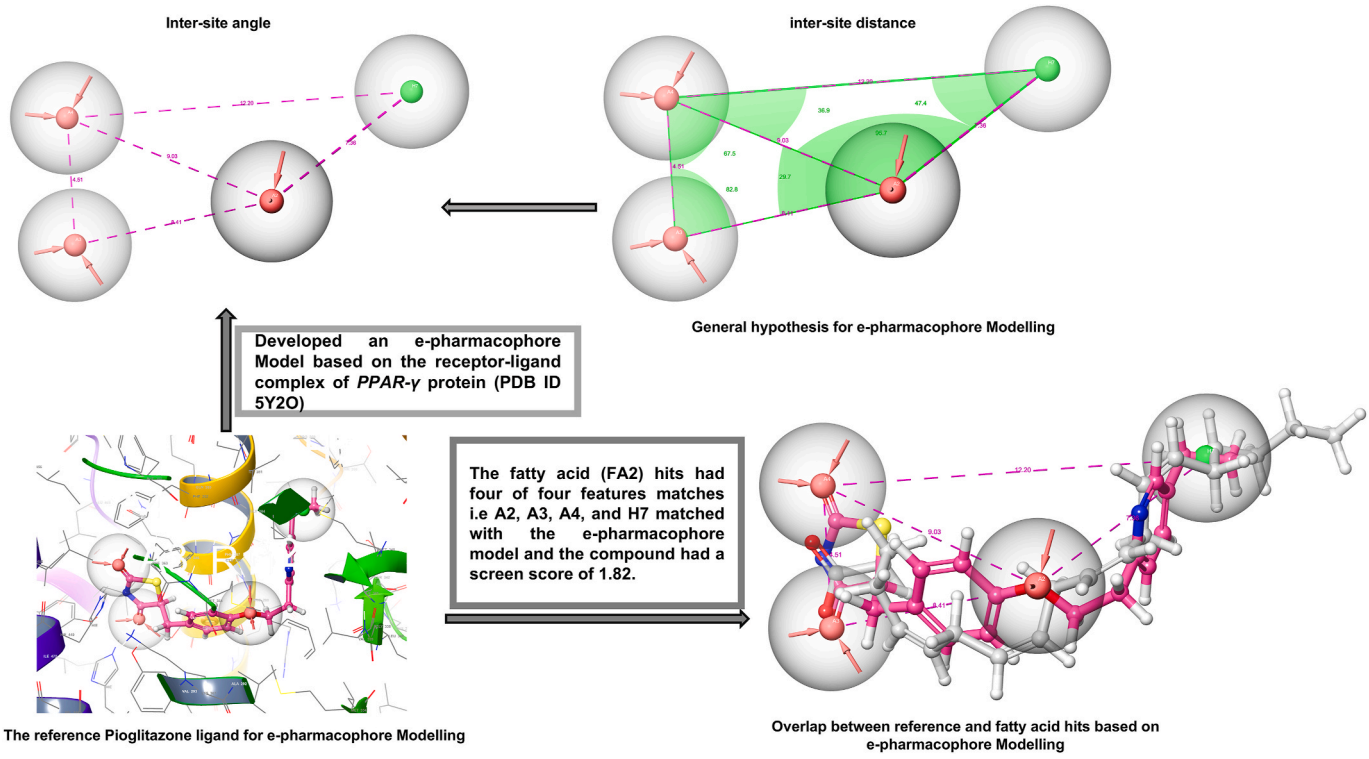

Fig. 9. e-Pharmacophore-based design strategy of fatty acids as potential *PPAR-γ* agonists.

Table 1
Score of e-Pharmacophore hypothesis model.

Code	Align Score	Vector Score	Volume Score	PhaseScreenScore
Pioglitazone	0.94	0.64	0.67	1.97
FA2	0.86	0.57	0.54	1.82
FA1	0.81	0.55	0.52	1.62
FA4	0.76	0.42	0.52	1.33
FA3	0.72	0.43	0.50	1.32

3.5. Molecular dynamic simulations

3.5.1. Intermolecular interactions in molecular dynamics simulation

A 100 ns molecular dynamics simulation using the Desmond program was performed to investigate the stability and conformational dynamics of specific inhibitors within the binding pockets of PPAR-δ/γ proteins. The study evaluated key parameters, including Root Mean Square Deviation (RMSD), Root Mean Square Fluctuation (RMSF), and hydrogen bond interactions, to assess the intermolecular interactions and structural behavior of both the protein and ligand.

For compound FA1, the protein-ligand RMSD plot revealed distinct conformational changes compared to the initial reference structure. The protein RMSD values were 2.020 Å for the C-alpha atoms and 2.098 Å for the backbone, with maximum deviation observed at frame 104. Ligand stability analysis showed maximum RMSD deviations of 2.681 Å when aligned on the protein and 1.551 Å when aligned on the ligand, occurring at frame 65. RMSF analysis identified TYR473 as the most fluctuating residue in the PPAR-γ protein, with RMSF values of 0.940 Å (C-alpha) and 1.048 Å (backbone), peaking at frame 260 (Fig. 12). The ligand RMSF values were 1.583 Å (aligned on the protein) and 1.559 Å (aligned on the ligand), with the highest fluctuation at frame 17, indicating dynamic behavior in the binding pocket and the adaptability of the inhibitors (Fig. S7).

In the case of compound FA2, the protein RMSD values were 2.074 Å for the C-alpha atoms and 2.030 Å for the backbone, with the maximum deviation occurring at frame 312. Ligand RMSD values highlighted

Table 2
Binding affinity and interactions of fatty acids (FA1 to FA4) using Glide module of Schrodinger's.

Comp.	Docking Score (XP)	Glide Energy (Kcal/mol)	Ligand Atom Hydrogen bond interactions	Bond Length (Å)
***PPAR-γ* binding pocket (PDB ID:** 5Y2O)				
FA1	−8.14	−39.24	- O of ligand to TYR 473, HIE 323, HIE449, and SER289	1.91 2.18 1.23 1.21
FA2	−8.02	−37.05	-O of ligand to TYR 473, HIE 323, HIE449, and SER289	1.20 1.27 1.45 1.24
FA3	−6.99	−32.34	-O of ligand to HIE 323, HIE449, and SER289	2.18 1.02 1.14
FA4	−6.98	−30.22	-O of ligand to HIE 323, HIE449, and SER289	1.31 1.02 1.07
Pioglitazone/ 8N6	−10.57	−59.11	-O of ligand to TYR473, SER289 and HIE323	2.12 2.03 3.23
PPAR-δ binding pocket (PDB ID: 3GZ9)				
FA1	−9.64	−35.74	-O of ligand to TYR 473, and HIE449	1.23 1.21
FA2	−11.03	−41.11	-O of ligand to TYR 473, HIE 323, and HIE449	1.24 1.52 1.26
FA3	−9.10	−37.88	-O of ligand to TYR 473, HIE 323, and HIE449	1.71 1.24 1.05
FA4	−8.87	−32.69	-O of ligand to TYR 473, and HIE449	2.14 1.25
D32	−10.57	−59.11	-O of ligand to TYR473, SER289, THR288 and HIE323	2.12 2.03 3.23 1.24

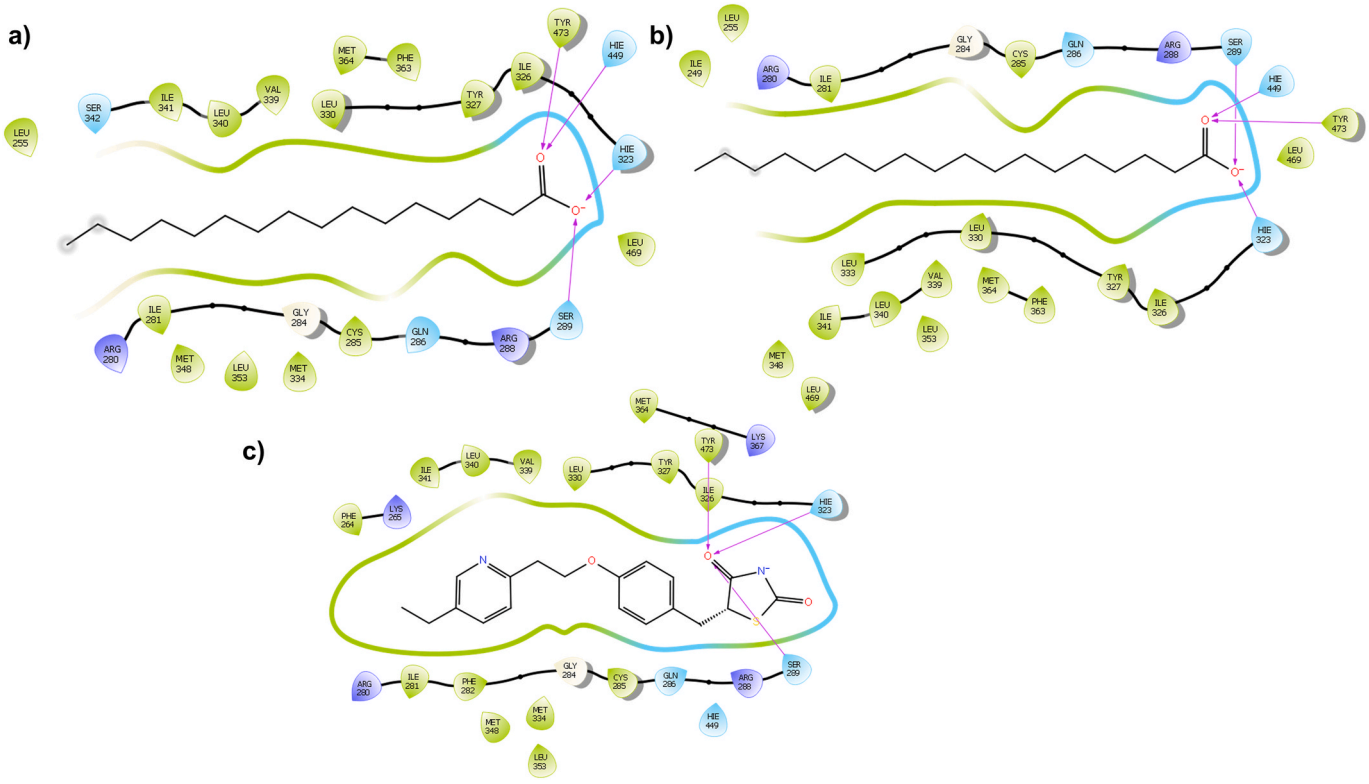

Fig. 10. Orientation of fatty acids a) FA1, b) FA2 and c) Pioglitazone in crystal structure of PPAR-γ binding pocket.

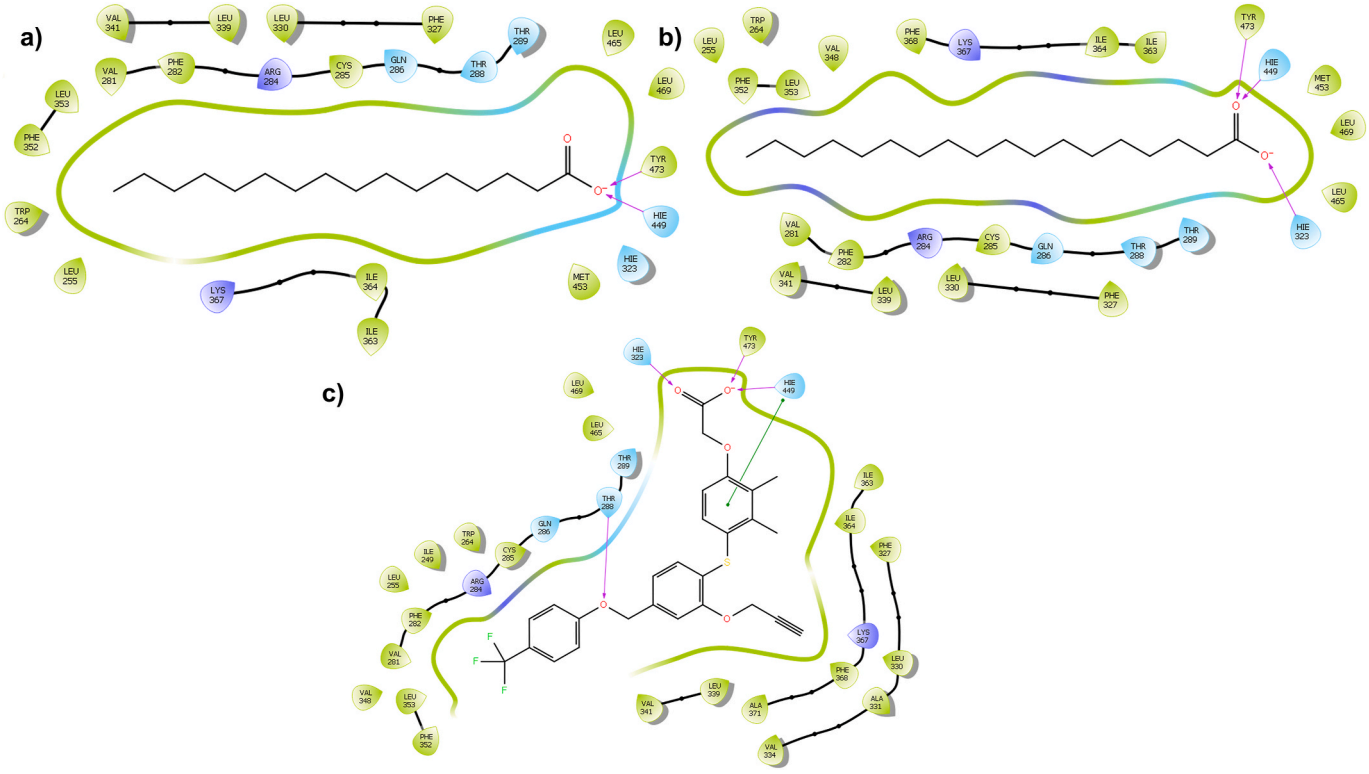

Fig. 11. Orientation of fatty acids a) FA1, b) FA2 and c) D32 in crystal structure of PPAR-δ binding pocket.

deviations of 2.792 Å (aligned on the protein) and 1.997 Å (aligned on the ligand), with peak deviations at frame 11. RMSF analysis showed significant fluctuations in TYR473, with RMSF values of 1.495 Å (C-alpha) and 1.523 Å (backbone), peaking at frame 260. The ligand exhibited dynamic fluctuations, with RMSF values of 2.368 Å (aligned on the protein) and 1.430 Å (aligned on the ligand), reaching maximum

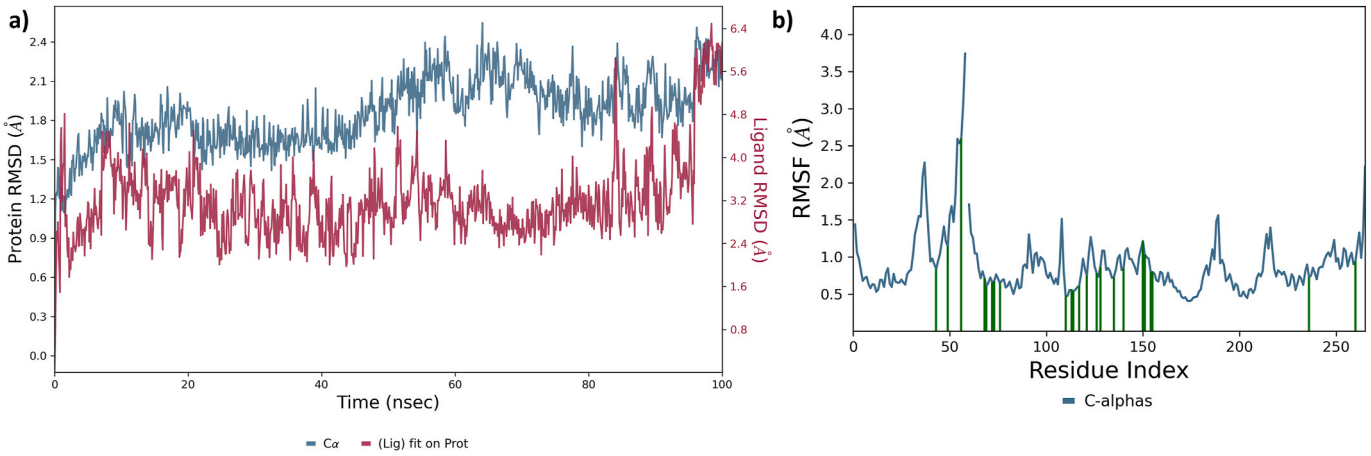

Fig. 12. (a) Protein Ligand RMSD Plot of FA1, (b) Protein RMSF Plot over period of 100 ns within PPAR-γ protein.

fluctuation at frame 20. These observations suggest that compound FA2 demonstrates notable interaction and mobility within the PPAR-γ binding pocket (Fig. S6).

For compound FA2, the RMSD values for the protein structure were 2.044 Å for C-alpha and 2.027 Å for the backbone, with the maximum deviation at frame 152. Ligand stability was assessed with RMSD deviations of 2.286 Å (aligned on the protein) and 1.345 Å (aligned on the ligand) at frame 71. The RMSF plot for compound FA2 showed the highest fluctuations in TYR473, with RMSF values of 1.353 Å (C-alpha) and 1.562 Å (backbone) at frame 267. The ligand RMSF values were 1.456 Å (aligned on the protein) and 1.313 Å (aligned on the ligand) at frame 19, indicating notable fluctuations in the PPAR-δ binding pocket (Fig. 13).

For compound FA3, protein RMSD values were slightly higher, at 2.214 Å for the C-alpha atoms and 2.127 Å for the backbone, with the maximum deviation noted at frame 157. Ligand RMSD values were 2.286 Å (aligned on the protein) and 1.345 Å (aligned on the ligand), peaking at frame 71. RMSF analysis again highlighted TYR473 as the most dynamic residue, with RMSF values of 1.423 Å (C-alpha) and 1.652 Å (backbone), peaking at frame 263. The ligand showed RMSF values of 1.556 Å (aligned on the protein) and 1.403 Å (aligned on the ligand), with the highest fluctuation at frame 18, indicating significant interactions and structural adjustments within the PPAR-δ binding site (Fig. S6).

The molecular dynamics simulation results underscore the critical role of intermolecular interactions in maintaining the stability and adaptability of protein-ligand complexes. Residue TYR473 was consistently identified as a hotspot of fluctuation across all molecules, reflecting its importance in binding pocket dynamics. The observed RMSD and RMSF values highlight the conformational flexibility and binding behaviours of the inhibitors, offering valuable insights into their potential as modulators of PPAR-δ/γ activity.

3.5.2. *Intermolecular interactions in molecular dynamics simulation*

Fig. 14 displays a stacked bar chart that illustrates the intermolecular interactions between inhibitors and the PPAR-δ/γ protein during the molecular dynamic's simulation. The interactions are categorized into hydrogen bonds, hydrophobic interactions, ionic interactions, and water bridges, providing detailed insights into the dynamic behavior of each molecule within the binding pocket.

Compound FA2 exhibited a robust binding profile, forming hydrogen bonds with HIS323, HIS449, TYR473, hydrogen bonds and water bridges with GLN286, THR289, as well as hydrophobic interactions with LEU255, PHE282, CYS285, LEU339, ILE363. The 2D interaction diagram further emphasizes its polar interaction with HIS449, HIS323, TYR473, and water bridge with THR289.

Compound FA2 exhibited a robust binding profile, forming hydrogen bonds with THR289, HIS323, HIS449, TYR473, as well as hydrophobic interactions with VAL334, PHE368. The 2D interaction diagram further emphasizes its polar interaction with HIS449, HIS323, TYR473, THR289, reinforcing its stability and diverse binding interactions within PPAR-δ active pocket.

Compound FA1 exhibited a robust binding profile, forming hydrogen bonds and water bridges with SER289, HIS323, TYR327, TYR473, as well as hydrophobic interactions with LEU330, MET334, ILE341, MET348. The 2D interaction diagram further emphasizes its polar

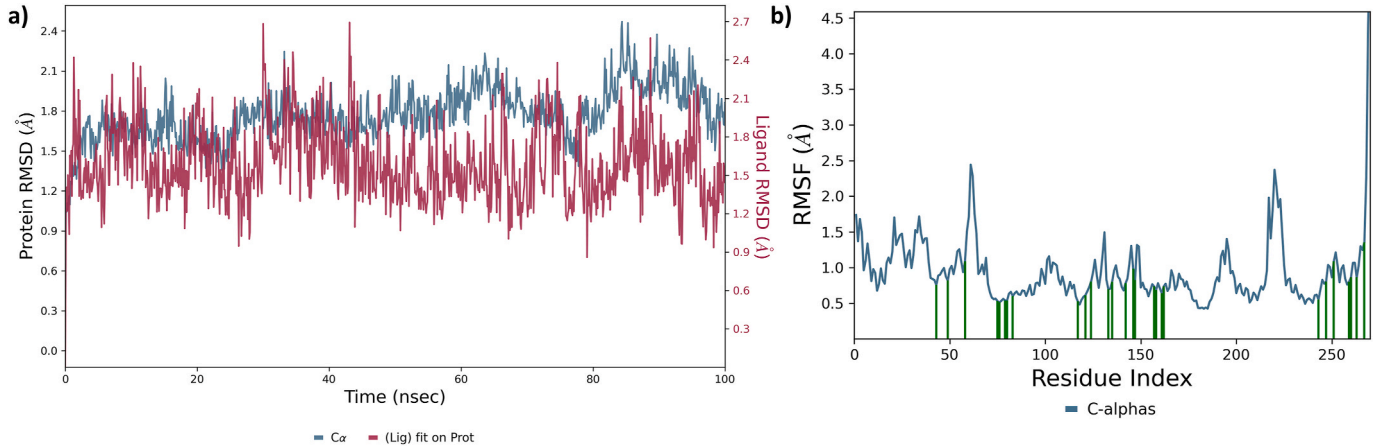

Fig. 13. (a) Protein Ligand RMSD Plot of FA2, (b) Protein RMSF Plot over period of 100 ns within PPAR-δ protein.

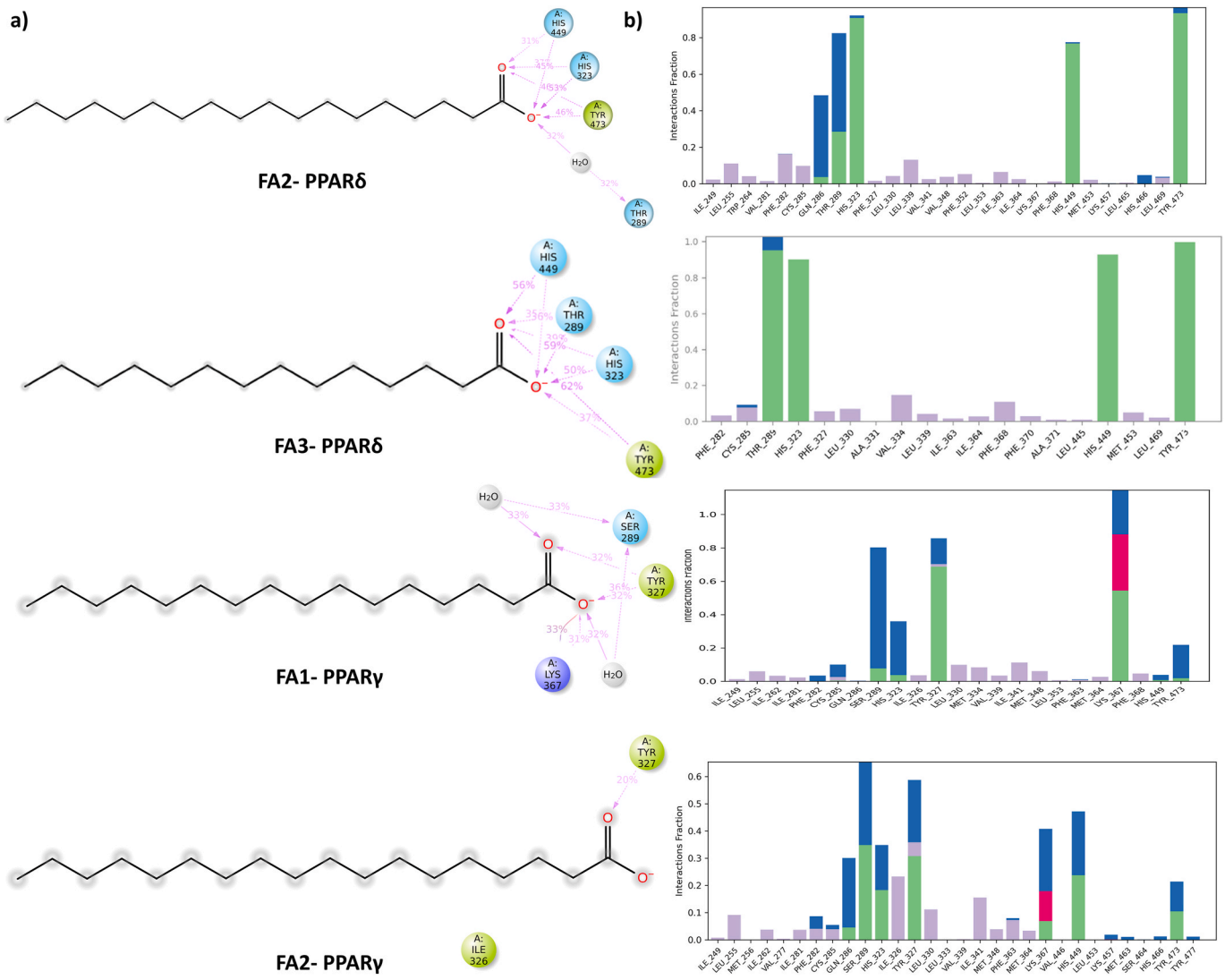

Fig. 14. (a) Ligand protein contacts with the respective amino acids, b) Protein ligand contacts of molecules with the respective amino acids of the protein of the PPAR-δ/γ protein.

interaction with TYR327, water bridge with SER289, and salt bridge with LYS367, reinforcing its stability and diverse binding interactions within PPAR-γ active pocket.

Compound FA2 exhibited a robust binding profile, forming hydrogen bonds and water bridges with GLN286, SER289, HIS323, TYR327, HIS449, TYR473, as well as hydrophobic interactions with LEU255, ILE326, LEU330, ILE341, MET348, PHE363. The 2D interaction diagram further emphasizes its polar interaction with TYR327, reinforcing its stability and diverse binding interactions within PPAR-γ active pocket. In summary, both compounds demonstrated robust and diverse binding interactions with PPAR-δ/γ proteins, with FA2 showing particularly strong polar and hydrophobic interactions that reinforce its stability and potential efficacy within the active sites.

3.6. Density functional theory (DFT) analysis

3.6.1. Optimization of molecular geometries

Table 4 provides a detailed summary of the optimization parameters for fatty acid molecular structures, encompassing total energy and gas-phase energy. The structural and electronic properties of these fatty acids were analyzed using quantum chemical calculations to understand their chemical behavior. Molecular orbitals, particularly the highest occupied molecular orbital (HOMO) and the lowest unoccupied molecular orbital (LUMO), are pivotal in elucidating reactivity, stability, and kinetic properties.

The energy gap (ΔEGAP), a critical descriptor of chemical reactivity, was calculated alongside other quantum descriptors using the DFT/B3LYP/6-31G (d, p**) method. As shown in Table 3, compounds FA1, FA2, FA3, and FA4 exhibit varying electronic properties, with FA3 demonstrating the smallest ΔEGAP (0.141 eV). This smaller gap indicates that FA3 has the highest reactivity and the lowest molecular hardness (η), which is directly proportional to the molecule's resistance to reactivity or deformation. Consequently, FA3 emerges as the softest and most reactive compound in the series, as evidenced by its hardness value ($\eta = 0.070526$eV) and a high softness ($\sigma = 14.179$eV). Additional reactivity descriptors, including chemical potential (μ) and electrophilicity index (ω), further illustrate the electronic behavior of the

Table 3
Final Energy of Geometry optimized structures.

Compound	Gas Phase Energy (eV)	ESP min, kcal/mol
FA1	−779.520	−33.11
FA2	−858.150	−34.84
FA3	−700.305	−157.53
FA4	−622.255	−35.52

Table 4
Calculated quantum chemical parameters of fatty acid molecules Molecular electrostatic Potential Surface.

Quantum chemical parameters	FA1	FA2	FA3	FA4
E_{HOMO} (eV)	−0.273949	−0.269437	−0.004781	−0.267327
E_{LUMO} (eV)	0.010703	0.009775	0.136271	0.012921
ΔE_{GAP} (eV)	0.284652	0.279212	0.141052	0.280248
η (eV)	0.142326	0.139606	0.070526	0.140124
μ (eV)	−0.131623	−0.129831	0.065745	−0.127203
ω (eV)	0.060862	0.060370	0.030644	0.057737
σ (eV)	7.026123	7.163016	14.179168	7.136536

compounds. FA3 displays a chemical potential of 0.065745eV and an electrophilicity index of 0.030644 eV suggesting enhanced reactivity compared to the other fatty acids. Electrostatic potential (ESP) mapping was performed to visualize regions of high (negative) and low (positive) electron density across the molecular structures. These regions are instrumental in predicting sites susceptible to electrophilic and nucleophilic attacks. Using optimized geometries within the B3LYP/6-31G (d, p**) framework, the ESP maps (Fig. 15) and the results presented in Table 4 reveal critical interaction sites, offering valuable insights into the molecular dynamics of fatty acids.

3.7. ADME predictions

The ADME properties of fatty acid molecules (FA1–FA4) were evaluated using Schrödinger's QikProp module, focusing on key pharmacokinetic and physicochemical parameters essential for drug development (Table S1). The analysis assessed properties such as lipophilicity (QPlog Po/W), solubility (QPlogS), polar surface area (PSA), permeability (Caco-2 and MDCK assays), binding affinity to human serum albumin (QPlog Khsa), blood-brain barrier penetration (QPlog BB), human oral absorption (HOA), and compliance with drug-likeness rules (Lipinski's Rule of Five and Jorgensen's Rule of Three). The findings, summarized below, highlight the potential of these molecules for further development.

The molecules exhibited strong lipophilicity, with QPlog Po/W values of 5.22 (FA1), 6.00 (FA2), 4.50 (FA3), and 3.75 (FA4), indicating excellent partitioning behavior in biological systems. Despite their favorable lipophilicity, the compounds displayed poor aqueous solubility, as indicated by QPlogS values of −5.41 (FA1), −6.33 (FA2), −4.67 (FA3), and −3.70 (FA4), which fall outside the acceptable range (−3.70 to −6.33). This suggests a potential challenge in achieving adequate solubility during formulation. Permeability assessments revealed promising outcomes. The MDCK assay results ranged from 131.34 nm/s (FA2) to 158.31 nm/s (FA4), while Caco-2 permeability values ranged from 234.71 nm/s (FA2) to 278.97 nm/s (FA4), indicating excellent membrane permeability for all molecules. Human oral absorption (HOA) predictions further corroborated their strong pharmacokinetic profiles, with FA1, FA3, and FA4 achieving a 3 rating (corresponding to 100 % absorption) and FA2 achieving a 1 rating. Additional evaluations included QPlog Khsa values, which ranged from 0.031 (FA4) to 0.778 (FA2), reflecting favorable binding affinity to human serum albumin. The QPlog BB values ranged from −1.45 (FA1) to −1.02 (FA4), suggesting moderate blood-brain barrier penetration potential. The polar surface area (PSA) values were consistent across the series, around 50 $Å^2$, supporting balanced permeability and transport characteristics. All molecules complied with Lipinski's Rule of Five (RoF) and Jorgensen's Rule of Three (RoT), confirming their drug-likeness. The hydrogen bond acceptor (HBA) and donor (HBD) counts were within acceptable ranges, with all molecules having two HBAs and one HBD, indicating favorable hydrogen bonding potential. The solvent-accessible surface area (SASA) values varied from 538.13 $Å^2$ (FA4) to 733.19 $Å^2$ (FA2), further supporting their favorable pharmacokinetic attributes.

4. Discussion

This study aimed to investigate the potential of fatty acids as therapeutic agents for diabetes mellitus. Initially, 12 fatty acids (FA1-FA12) were subjected to network pharmacology analysis to identify their interactions with proteins and pathways associated with the disease. This analysis revealed that these compounds modulate key targets involved in diabetes, such as PPAR, GAA, INSR, SLC2A4, PPARD, MAPK1, and AKT1, suggesting their potential to influence multiple biological pathways. To further refine the analysis, a structure-based pharmacophore model was generated using the PPAR-γ protein and its inhibitor, Pioglitazone, as a reference. This model identified key structural features required for effective binding and activity at the PPAR-γ receptor. Based

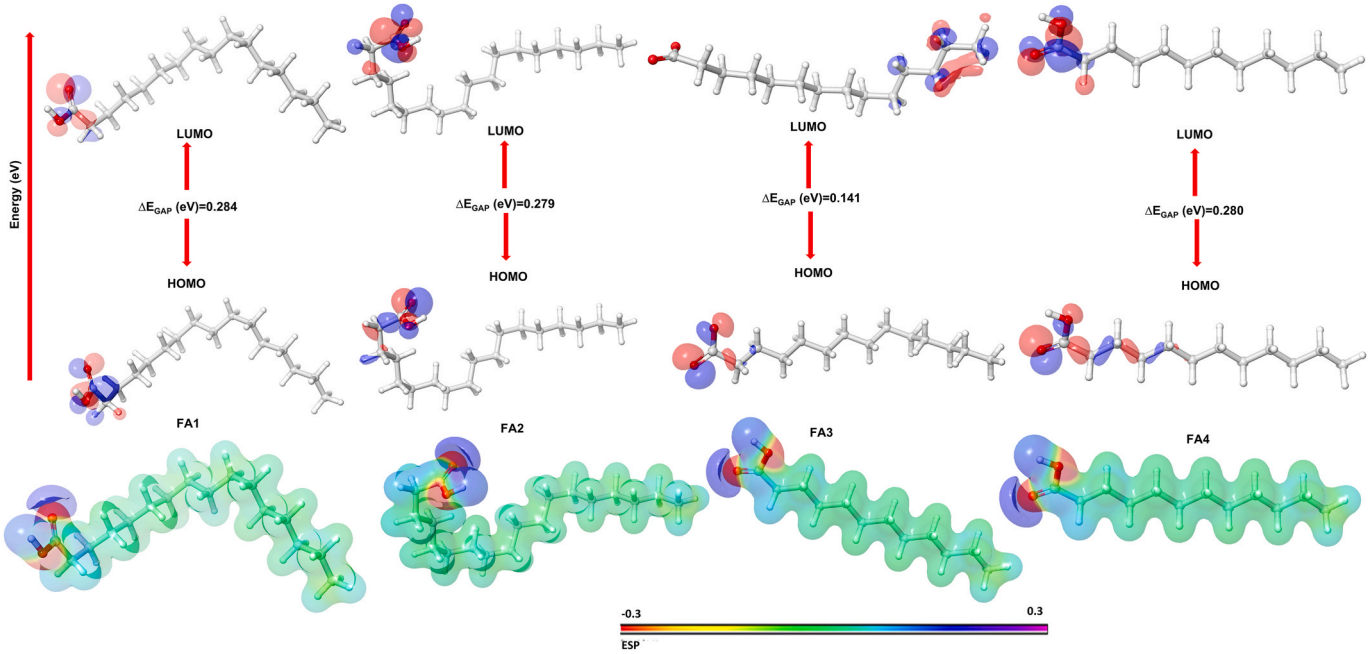

Fig. 15. Contours of HOMO, LUMO and ESP of FA1 to FA4.

on this model, the 12 initial fatty acids were filtered, and the top 4 (FA1-FA4) were selected for further investigation. Molecular docking studies were then performed on these four selected fatty acids against PPAR-γ and PPAR-δ. The results showed that FA1 and FA2 exhibited the most favorable binding affinities and interactions within the active sites of both receptors. Key amino acid residues, such as TYR473, HIE323, and HIE449, were found to be crucial for binding stability within the active pockets of both receptors. Finally, density functional theory (DFT) calculations were performed to assess the electronic properties of the selected fatty acids. These calculations revealed that FA3 exhibited the highest reactivity and the lowest molecular hardness, suggesting enhanced reactivity compared to the other fatty acids. Furthermore, all four fatty acids demonstrated favorable pharmacokinetic properties, including good lipophilicity, permeability, and compliance with drug-likeness rules. In conclusion, this study provides valuable insights into the potential of fatty acids as modulators of lipid-sensing nuclear receptors PPARδ/γ for glycemic regulation. The findings suggest that these compounds, particularly FA1 and FA2, may have therapeutic potential for diabetes mellitus by targeting key pathways involved in insulin signaling and glucose metabolism. Fatty acid-based therapies face limitations such as poor bioavailability, metabolic variability, and lack of potency compared to synthetic PPAR agonists (Đanić M et al., 2018). These challenges can be overcome by structural modifications, formulation advancements (e.g., nano-delivery systems), and combining fatty acids with existing therapies to enhance efficacy and stability.

5. Conclusion

This study comprehensively explored the therapeutic potential of fatty acids (FA1-FA12) in managing diabetes mellitus by targeting lipid-sensing nuclear receptors PPAR-γ and PPAR-δ. Network pharmacology and protein-protein interaction (PPI) analyses highlighted key pathways, including PI3K-Akt, MAPK, and insulin signaling, emphasizing their role in glucose homeostasis. To ensure a robust computational analysis, pioglitazone was used as a positive control, while all 12 fatty acids (FA1-FA12) served as potential negative controls in the structure-based drug design (SBDD) approach. A four-feature (HAAA) e-pharmacophore model was developed using the PPAR-γ crystal structure (PDB ID: 5Y2O) with pioglitazone (8N6) as a reference, enabling the identification of key ligand-receptor interactions. Molecular docking and MD simulations further confirmed that FA1 (Palmitic acid) and FA2 (Myristic acid) exhibited strong binding affinities and stable interactions at the PPAR-γ and PPAR-δ active sites. Free energy calculations distinguished the active fatty acids from the negative controls, reinforcing their potential role in improving insulin sensitivity and lipid metabolism. While these findings support the therapeutic potential of FA1 and FA2, further in vitro and in vivo validation is essential to confirm their efficacy and safety. Additionally, formulation strategies addressing solubility limitations will be necessary for potential clinical applications. This study establishes a strong foundation for developing lipid-sensing nuclear receptor modulators as novel therapeutic strategies for diabetes management.

CRediT authorship contribution statement

Shankar Gharge: Writing – review & editing, Writing – original draft, Visualization, Validation, Supervision, Project administration, Methodology, Investigation, Formal analysis, Conceptualization. **Charushila V. Balikai:** Resources. **Sachin Gudasi:** Software, Resources.

Funding sources

No funding was obtained for this study.

Declaration of competing interest

The authors declare that they have no known competing, financial interests or personal relationship that could have appeared to influence the work reported in this paper.

Acknowledgements

This work was supported by Department of Pharmaceutical chemistry, KLE College of Pharmacy, KLE Academy of Higher Education and Research, Belagavi and Department of Chemistry, SKE Society's Govindram Seksaria Science College, Belagavi-590006, Karnataka, India.

Appendix A. Supplementary data

Supplementary data to this article can be found online at https://doi.org/10.1016/j.amolm.2025.100079.

References

Agbu, P., Carthew, R.W., 2021. MicroRNA-mediated regulation of glucose and lipid metabolism. Nat. Rev. Mol. Cell Biol. 22, 425–438. https://doi.org/10.1038/s41580-021-00354-w.

Burdge, G.C., Calder, P.C., 2015. Introduction to fatty acids and lipids. ILE 112, 1–6. https://doi.org/10.1159/000365423.

DeFronzo, R.A., Ferrannini, E., Groop, L., Henry, R.R., Herman, W.H., Holst, J.J., Hu, F. B., Kahn, C.R., Raz, I., Shulman, G.I., Simonson, D.C., 2015. Type 2 diabetes mellitus. Nat. Rev. Dis. Primers 1, 1–22. https://doi.org/10.1038/nrdp.2015.19.

Ding, W., Liu, H., Qin, Z., Liu, M., Zheng, M., Cai, D., Liu, J., 2021. Dietary antioxidant anthocyanins mitigate type II diabetes through improving the disorder of glycometabolism and insulin resistance. J. Agric. Food Chem. 69, 13350–13363. https://doi.org/10.1021/acs.jafc.1c05630.

Đanić, M., Stanimirov, B., Pavlović, N., Goločorbin-Kon, S., Al-Salami, H., Stankov, K., Mikov, M., 2018. Pharmacological applications of bile acids and their derivatives in the treatment of metabolic syndrome. Front. Pharmacol. 9, 1382. https://doi.org/10.3389/fphar.2018.01382.

Falomir-Lockhart, L.J., Cavazzutti, G.F., Giménez, E., Toscani, A.M., 2019. Fatty acid signaling mechanisms in neural cells: fatty acid receptors. Front. Cell. Neurosci. 13, 162. https://doi.org/10.3389/fncel.2019.00162.

Festuccia, W.T., Blanchard, P.G., Deshaies, Y., 2011. Control of brown adipose tissue glucose and lipid metabolism by PPARγ. Front. Endocrinol. 2, 84. https://doi.org/10.3389/fendo.2011.00084.

Forouhi, N.G., Wareham, N.J., 2010. Epidemiology of diabetes. Médica Sur 11, 602–606. https://doi.org/10.1016/j.mpmed.2010.08.007.

Gharge, S., Alegaon, S.G., 2024. Recent studies of nitrogen and sulfur-containing heterocyclic analogues as novel antidiabetic agents: a review. Chem. Biodivers. 21, e202301738. https://doi.org/10.1002/cbdv.202301738.

Gharge, S., Alegaon, S.G., Jadhav, S., Ranade, S.D., Kavalapure, R.S., 2024a. Design, synthesis, characterization and antidiabetic evaluation of 3,5-substituted thiazolidinediones: evidenced by network pharmacology, molecular docking, dynamic simulation, in vitro and in vivo assessment. EJMCR. 12, 100213. https://doi.org/10.1016/j.ejmcr.2024.100213.

Gharge, S., Alegaon, S.G., Ranade, S.D., Kavalapure, R.S., Kumar, B.P., Mhaske, P.C., 2024b. Expression of PPAR-γ TF by newly synthesized thiazolidine-2,4-diones to manage glycemic control: insights from in silico, in vitro and experimental pharmacology in Wistar rats. Bioorg. Chem. 153, 107966. https://doi.org/10.1016/j.bioorg.2024.107966.

Gharge, S., Alegaon, S.G., Ranade, S.D., Khatib, N.A., Kavalapure, R.S., Kumar, B.P., Vinod, D., Bavage, N.B., 2024c. Design, synthesis of new 2,4-thiazolidinediones: in silico, in vivo anti-diabetic and anti-inflammatory evaluation. EJMCR 11, 100151. https://doi.org/10.1016/j.ejmcr.2024.100151.

Gharge, S., Alegaon, S.G., Ranade, S.D., Kavalapure, R.S., Kumar, B.P., 2025. Novel rhodanine–thiazole hybrids as potential antidiabetic agents: a structure-based drug design approach. RSC Med. Chem. https://doi.org/10.1039/D4MD00689E.

Gong, L., Wei, F., Gonzalez, F.J., Li, G., 2023. Hepatic fibrosis: targeting peroxisome proliferator-activated receptor alpha from mechanism to medicines. Hepatology 78, 1625–1653. https://doi.org/10.1097/HEP.0000000000000182.

Gudasi, S., Gharge, S., Koli, R., Kagawad, P., 2024. Exploring in silico, in vitro antioxidant, and cytotoxic potential of Valerian wallichii on cervical epithelial carcinoma (HeLa) cell lines. Chem. Biodiversity 21, e202302072.

Gudasi, S., Gharge, S., Koli, R., Patil, K., 2023. Antioxidant properties and cytotoxic effects of Oxalis corniculata on human Hepatocarcinoma (Hep-G2) cell line: an in vitro and in silico evaluation. Futur. J. Pharm. Sci. 9, 25. https://doi.org/10.1186/s43094-023-00476-2.

Kaltenecker, D., Themanns, M., Mueller, K.M., Spirk, K., Suske, T., Merkel, O., Kenner, L., Luís, A., Kozlov, A., Haybaeck, J., Müller, M., 2019. Hepatic growth hormone-JAK2-STAT5 signaling: metabolic function, non-alcoholic fatty liver disease, and hepatocellular carcinoma progression. Cytokine 124, 154569. https://doi.org/10.1016/j.cyto.2018.10.010.

Kavalapure, R.S., Alegaon, S.G., Venkatasubramanian, U., Priya, A.S., Ranade, S.D., Khanal, P., Mishra, S., Patil, D., Salve, P.S., Jalalpure, S.S., 2021. Design, synthesis, and molecular docking study of some 2-((7-chloroquinolin-4-yl) amino) benzohydrazide Schiff bases as potential Eg5 inhibitory agents. Bioorg. Chem. 116, 105381. https://doi.org/10.1016/j.bioorg.2021.105381.

Lampropoulou, I.T., Stangou, M., Sarafidis, P., Gouliovaki, A., Giamalis, P., Tsouchnikas, I., Didangelos, T., Papagianni, A., 2020. TNF-α pathway and T-cell immunity are activated early during the development of diabetic nephropathy in type II diabetes mellitus. Clin. Immunol. 215, 108423. https://doi.org/10.1016/j.clim.2020.108423.

Mackenzie, R.W., Elliott, B.T., 2014. Akt/PKB activation and insulin signaling: a novel insulin signaling pathway in the treatment of type 2 diabetes. Diabetes, Metab. Syndrome Obes. Targets Ther. 55–64. https://doi.org/10.2147/DMSO.S48260.

Maiese, K., 2015. FoxO transcription factors and regenerative pathways in diabetes mellitus. CNR 12, 404–413.

Marx, N., Duez, H., Fruchart, J.C., Staels, B., 2004. Peroxisome proliferator-activated receptors and atherogenesis: regulators of gene expression in vascular cells. Circ. Res. 94, 1168–1178. https://doi.org/10.1161/01.RES.0000127122.22685.0A.

Mauricio, D., Alonso, N., Gratacòs, M., 2020. Chronic diabetes complications: the need to move beyond classical concepts. Trends Endocrinol. Metabol. 31, 287–295. https://doi.org/10.1016/j.tem.2020.01.007.

McGillicuddy, F.C., Roche, H.M., 2012. Nutritional status, genetic susceptibility, and insulin resistance important precedents to atherosclerosis. Mol. Nutr. Food Res. 56, 1173–1184. https://doi.org/10.1002/mnfr.201100785.

Mirza, A.Z., Althagafi, I.I., Shamshad, H., 2019. Role of PPAR receptor in different diseases and their ligands: physiological importance and clinical implications. Eur. J. Med. Chem. 166, 502–513. https://doi.org/10.1016/j.ejmech.2019.01.067.

Mortier, J., Rakers, C., Bermudez, M., Murgueitio, M.S., Riniker, S., Wolber, G., 2015. The impact of molecular dynamics on drug design: applications for the characterization of ligand–macromolecule complexes. Drug Discov. Today 20, 686–702. https://doi.org/10.1016/j.drudis.2015.01.003.

Palomer, X., Barroso, E., Pizarro-Delgado, J., Peña, L., Botteri, G., Zarei, M., Aguilar, D., Montori-Grau, M., Vázquez-Carrera, M., 2018. Pparβ/δ: a key therapeutic target in metabolic disorders. Int. J. Mol. Sci. 19, 913. https://doi.org/10.3390/ijms19030913.

Patil, S., Alegaon, S.G., Gharge, S., Ranade, S.D., Khatib, N.A., 2024. Molecular hybridization, synthesis, in vitro α-glucosidase inhibition, in vivo antidiabetic activity and computational studies of isatin-based compounds. Bioorg. Chem. 153, 107783. https://doi.org/10.1016/j.bioorg.2024.107783.

Ranade, S.D., Alegaon, S.G., Khatib, N.A., Gharge, S., Kavalapure, R.S., 2024a. Quinoline-based Schiff bases as possible antidiabetic agents: ligand-based pharmacophore modeling, 3D QSAR, docking, and molecular dynamics simulations study. RSC Med. Chem. 15, 3162–3179. https://doi.org/10.1039/D4MD00344F.

Ranade, S.D., Alegaon, S.G., Khatib, N.A., Gharge, S., Kavalapure, R.S., Kumar, B.P., 2024b. Design, synthesis, molecular dynamic simulation, DFT analysis, computational pharmacology and decoding the antidiabetic molecular mechanism of sulphonamide-thiazolidin-4-one hybrids. J. Mol. Struct. 1311, 138359. https://doi.org/10.1016/j.molstruc.2024.138359.

Ranade, S.D., Alegaon, S.G., Khatib, N.A., Gharge, S., Kavalapure, R.S., Kumar, B.P., 2024c. Reversal of insulin resistance to combat type 2 diabetes mellitus by newer thiazolidinediones in fructose-induced insulin-resistant rats. Eur. J. Med. Chem. 280, 116939. https://doi.org/10.1016/j.ejmech.2024.116939.

Shen, H., Ding, L., Baig, M., Tian, J., Wang, Y., Huang, W., 2021. Improving glucose and lipids metabolism: drug development based on bile acid related targets. CESPEDESIA 5, 1. https://doi.org/10.15698/cst2021.01.239.

Spector, A.A., 1999. Essentiality of fatty acids. Lipids 34, S1–S3. https://doi.org/10.1007/BF02562220.

Villacorta, L., Schopfer, F.J., Zhang, J., Freeman, B.A., Chen, Y.E., 2009. PPARγ and its ligands: therapeutic implications in cardiovascular disease. Clin. Sci. 116, 205–218. https://doi.org/10.1042/CS20080195.

Wang, H., Li, N., Chivese, T., Werfalli, M., Sun, H., Yuen, L., Hoegfeldt, C.A., Powe, C.E., Immanuel, J., Karuranga, S., Divakar, H., 2022. IDF diabetes atlas: estimation of global and regional gestational diabetes mellitus prevalence for 2021 by International Association of Diabetes in Pregnancy Study Group's Criteria. Diabetes Res. Clin. Pract. 183, 109050. https://doi.org/10.1016/j.diabres.2021.109050.

Yanamadala, V., 2024. Lipid metabolism. In: Essential Medical Biochemistry and Metabolic Disease: A Pocket Guide for Medical Students and Residents. Springer Nature Switzerland, Cham, pp. 35–90. https://doi.org/10.1007/978-3-031-59394-9_2.